Optical Engineering

SPIEDigitalLibrary.org/oe

Design of an interferometric system for gauge block calibration

Javier Diz-Bugarín
Benito V. Dorrío
Jesús Blanco
Marta Miranda
Ismael Outumuro
José Luis Valencia

Design of an interferometric system for gauge block calibration

Javier Diz-Bugarín
Benito V. Dorrío
Jesús Blanco
Marta Miranda
University of Vigo
Applied Physics Department
Campus Universitario
36310 Vigo, Spain
E-mail: jbugarin@uvigo.es

Ismael Outumuro
José Luis Valencia
Laboratorio Oficial de Metroloxía de Galicia
R&D Department, Parque Tecnolóxico de Galicia
32901 Ourense, Spain

Abstract. We have developed an interferometer for gauge block calibration based on phase shifting algorithms. The measurement process can provide flatness, parallelism, and length. Wavelength values need to be corrected according to the refractive index of air. This correction is obtained indirectly using Edlén's equation. High-resolution sensors provide the temperature, pressure, and relative humidity readings. To preserve stability, the interferometer is encapsulated in a chamber with active temperature control. Its design, measurement principle, calibration, stability, and reproducibility are analyzed. Since one goal is to employ robust and cheap diode lasers as light sources, we describe the system developed to stabilize a red laser diode using a mode locking technique with a reference gas cell. The instruments and assembly are used to avoid the Doppler effect in the gas cell, which would limit wavelength resolution. Several experiments are carried out to restrict the influence of environmental changes, which affect laser diode frequency. [DOI: 10.1117/1.OE.52.4.045601]

Subject terms: phase shifting; gauge block; optical standards and testing; metrology; external cavity diode laser; iodine cell.

Paper 130130P received Jan. 24, 2013; revised manuscript received Mar. 6, 2013; accepted for publication Mar. 12, 2013; published online Apr. 3, 2013.

1 Introduction

Procedures for ensuring industrial quality require metrological calibration processes that guarantee the traceability of the reference magnitudes for the measurement instruments. In dimensional metrology, gauge blocks (GBs) materialize the unit length or its submultiples, where the length of the GB is considered to be the perpendicular distance between two gauging surfaces. The traditional interferometric configuration used for this purpose employs two or more gas laser sources that are frequency stabilized, and it needs a housing capsule for the interferometric module with control over temperature, relative humidity, and atmospheric pressure (typical uncertainties are below 0.1°C in temperature, 1% in relative humidity, and 0.1 mbar in pressure).[1] These values are used to monitor the temperature of the measured GBs (at the reference temperature of 20ºC, according to ISO 3650:1998) and to calculate the air refractive index using a modified version of Edlén's equation,[2–4] because the refractive index determination is a crucial part of the gauge block calibration procedure.[5] To preserve the stability conditions, the interferometer is encapsulated within an insulated chamber with an active temperature control. Therefore, it is necessary to develop an electronic control system which manages the position of the GBs, the optical phase modulation, the image processing system, and the CCD camera to obtain the optical phase by means of the appropriate combination of the interferograms modulated in phase. Because they affect the measurement of the length, problems associated with this interferometric process should be also considered, such as variations in contact layer thickness, phase shift corrections, environmental variations, and geometrical deviations.

This work reports on the advance of the design and construction of an interferometric device, its thermostatic housing, and its refractometric module, paying attention to the operation and stability of the most determinant variables. Calibration of the optomechanical modulator is done by using differential phase shifting algorithms[6–8] (DPSAs), while the experimental values of the refractive index of air are compared with those provided by the National Institute of Standards and Technology[9] (NIST).

The experimental setup is related to the red diode laser stabilization using a mode-locking frequency technique, which is also presented. Since the results show a suitable frequency stabilization of the diode laser, this stabilized red laser diode will be integrated later in the interferometric optical phase evaluation system.

2 Principle of Measurement

Figure 1 shows the interferometer configuration employed to determine the GB's length. As can be seen, the GB is placed on a reference support surface (RSS) in such a way that the wavefronts reflected from the GB and the reference optical surface (ROS) coming from the other interferometric arm are superimposed. With this arrangement, the longitudinal length of the GB can be estimated by fractional excess[10] as a multiple of the semiwavelengths contained in its length. That is,

$$L = \frac{\lambda_1}{2}(m_1 + F_1) = \cdots = \frac{\lambda_j}{2}(m_j + F_j), \tag{1}$$

where L is the length of the GB, λ_j represents the laser wavelength, m_j represents a whole number of fringes, and F_j is

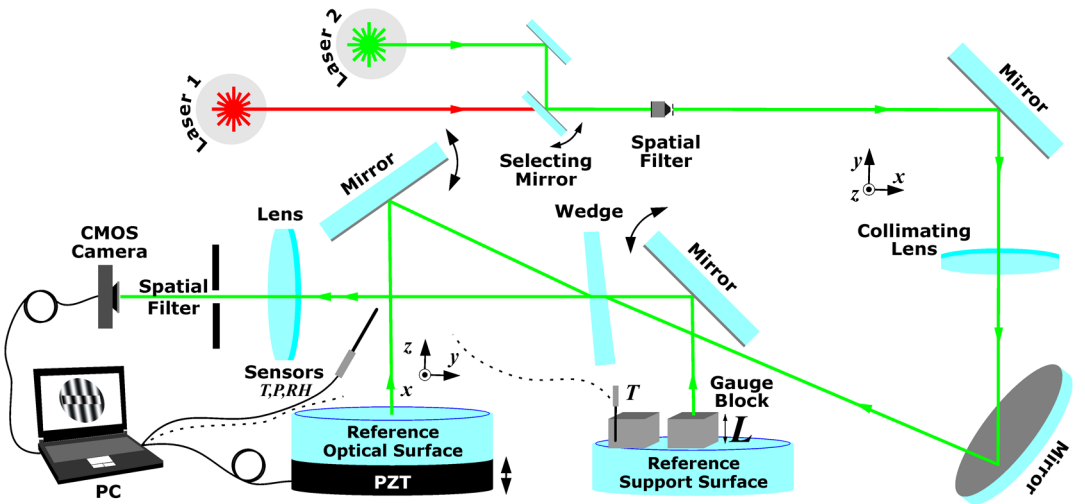

Fig. 1 This experimental setup uses the following principal elements: double He-Ne illumination (632.8 and 543.2 nm); Zerodur mirrors with a flatness of $\lambda/20$; 2M-XLI (CMOS-RGB) and Thorlabs-DCC1545M cameras; a PZT Physik Instrumente P-733.ZCL piezo nanopositioner; a Julabo F25MC circulator; an ASL 600 DC F600 thermometry bridge; and a Vaisala PTU 3030 barometer.

the fractional excess or the decimal part of these semiwavelengths. It is necessary to iterate the results obtained with several laser wavelengths, because a unique wavelength does not allow us to calculate the total number of semiwavelengths of the assessed GBs. This interferometric process requires the frequency stabilization of the laser to correct the theoretical wavelength of the source from vacuum to air values. Therefore, the refractive index [at temperatures near 20°C (68°F)] for each wavelength n_j of the interferometer is accurately controlled using Eldén's experimental equation[2–4] as

$$(n_j-1)\cdot 10^8 = \left(8342.54+\frac{2406147}{130-\lambda_j^{-2}}+\frac{15998}{38.9-\lambda_j^{-2}}\right)\cdot\left(\frac{P}{96095.43}\right)\left[\frac{1+10^{-8}(0.601-0.00972T)P}{1+0.0036610T}\right] - \mathrm{RH}(8.753+0.036588T^2)\times(0.037345-0.000401\lambda_j^{-2}), \quad (2)$$

once the temperature T, the atmospheric pressure P, and the relative humidity RH are known. The influence of the CO_2 composition is not considered. Ciddor's experimental equation[11] provides similar results at our working temperature, and it should give better results for the refractive index of air than Eq. (2) over a broader range of wavelengths and under severe environmental conditions of temperature, pressure, and humidity.[9]

What is more, the fractional excess is measured using the phase difference of the fringes formed on the GB with respect to those formed on the RSS[10] as

$$F_j = \frac{[\phi_{\mathrm{RSS}} - \phi_{\mathrm{GB}}]_j}{2\pi}. \quad (3)$$

This provides the interference fringe pattern that is shifted in phase by the modulation system, the computer-controlled PZT, obtaining a series of phase-shifted fringe patterns expressed as

$$s_m(\mathbf{r},\phi,\alpha_m) = a_0(\mathbf{r}) + a_1(\mathbf{r})\cos[\phi(\mathbf{r})+\alpha_m], \quad (4)$$

where $a_0(\mathbf{r})$ is the average local irradiance value, $a_1(\mathbf{r})$ is the modulation amplitude which is proportional to the visibility, and α_m is the additional introduced phase shift. This optical phase $\phi(\mathbf{r})$ is retrieved by using phase shift algorithms[12] (PSAs) as

$$\phi(\mathbf{r}) = \arctan\left[\sum_{m=1}^{M} n_m s_m(\mathbf{r},\phi,\alpha_m) \Big/ \sum_{m=1}^{M} d_m s_m(\mathbf{r},\phi,\alpha_m)\right], \quad (5)$$

where n_m and d_m are the coefficients of the corresponding PSA. The main error source during this process is given by the lack of repeatability of the piezoelectric system.

The measurement of a mechanical comparator is combined with the exact fractions calculation method to provide the final result, which is then completed with corrections such as heat dilatation, obliquity, or phase shift of different materials between the GB and the RSS. Uncertainty estimation associated with the determination of the GB's length indicate that thermal expansion due to the temperature gradient between the GB and its setting makes a contribution of more than 63% in the uncertainty evaluation.[13] It is therefore necessary to control the environmental parameters during the process of measurement. In this way, the GB's length is corrected from the measured temperature to the reference temperature of 20°C, according to its coefficient of linear thermal expansion, and taking into account possible phase shifts and obliquity errors.[1]

3 Interferometric System

The design implemented in this work is essentially a Twyman-Green interferometer (Fig. 1) at present, with a double He-Ne laser light source (632.8 and 543.2 nm) where the GB is illuminated vertically, according to the standard, and is wrung to the RSS. This surface and the ROS on the other arm of the interferometer are selected with good flatness and low wavefront distortion (Zerodur mirrors with $\lambda/20$ of flatness). Since our system provides

the optical and not the mechanical length, an error related to the different characteristics of the surfaces must be corrected. If two wavelengths are used, the length of the GB must be previously measured better than 1 μm. The collimation of the original beam is obtained with an achromatic doublet with a focal length of 500 mm, for a 2 in. optic, and with expansion possibilities. The light reflected from the ROS interferes with the light reflected from the GB and the RSS where the GB is wrung. For image acquisition, there is a choice of cameras: a 2M-XLI (CMOS-RGB) or a Thorlabs-DCC1545M (monochrome CMOS). Optomechanical modulation is carried out by a Physik Instrumente P-733.ZCL piezo nanopositioner with a displacement range of 100 μm and a nominal resolution of 0.3 nm. To adjust the fringe pattern (period and orientation), a fine adjustment is available. The control and evaluation system is made up of a main program written in C ++, which controls the different modules for positioning, acquisition, processing, and calculation of the optical phase (absolute/differential) in quasi-real-time using both conventional and custom designed PSAs/differential PSAs. The system also communicates with the atmospheric measuring equipment in order to include its readings in the calculation process. In the future, the modular design of the aforementioned program will allow us to insert or change its different components effortlessly.

There are two good reasons to control the environmental parameters around the GB and the interferometer. The first reason is to limit the temperature gradients between the block and its setting; the second reason is to monitor the air temperature, pressure, and relative humidity levels used to calculate the air refractive index. This requirement led us to encapsulate the measurement system in a thermostatic housing. Its structure is made up of modular aluminum profiles. Each wall is heat stabilized and is composed of a copper coil covered with insulation foam and sitting between two aluminum plates. This system was installed in the roof of the housing and in the four side walls, one of which is removable to access the inside of the interferometer. The housing is made up of an aluminum structure suitable for coupling to the mechanical base of the interferometer, which makes the assembly stable and secure. The walls are attached to this tubular aluminum structure by a custom designed system, and they act as heat exchangers between the copper coil and the inside the housing. In addition, we have installed a Julabo F25MC circulator with the nominal specification for PID controller stability. The required environmental values are monitored in real-time by a LabView® control program through an ASL 600 DC F600 thermometry bridge (uncertainty is higher than 10 ppm) and a Vaisala PTU3030 (uncertainties are higher than 0.1ºC in temperature, 1% in relative humidity, and 15 Pa in pressure). Readings are used for the indirect calculation of the refractive index of a specific wavelength according to Eq. (2). Figure 2 shows the evolution of the refractive index calculated over a period of 24 h. The measurement process was carried out in an environmentally controlled room at Laboratorio Oficial de Metroloxía de Galicia (LOMG) once the optical module was sealed and the additional temperature stabilization was allowed. To validate the implementation of our own software design, the results were compared with the reference results published by the NIST.[9] This comparison indicates a RMS deviation of 2.3 e-10, which is less than the ninth decimal of the refractive index. These values are compatible, bearing in mind that the uncertainty of the air refractive index and the experimental results exceed the eighth digit.

The calibration procedure consists of an acquisition of $M+N$ shifted patterns with known phase increments. A nominal control shift δ is introduced between the first M patterns, Eq. (4), and the δ-shifted N patterns (Fig. 3), such that

$$s_{M+m}(\mathbf{r},\phi,\alpha_{M+m}) = a_0(\mathbf{r}) + a_1(\mathbf{r})\cos[\phi(\mathbf{r}) + \delta_{\mathrm{PZT}} + \alpha_{M+m}]. \tag{6}$$

This process is repeated for consecutive increments of δ_{PZT}, and the phase difference between both patterns is recalculated, δ_{DPSA}, in each case with a DPSA[6–8] so that

$$\tan[(\phi+\delta_{\mathrm{DPSA}})-\phi] = \tan[\delta_{\mathrm{DPSA}}] = \frac{\sum_{m=1}^{M} d_m s_m(\mathbf{r},\phi,\alpha_m)\sum_{m=1}^{N} n_m s_{M+m}(\mathbf{r},\phi+\delta_{\mathrm{PZT}},\alpha_{M+m}) - \sum_{m=1}^{M} n_m s_m(\mathbf{r},\phi,\alpha_m)\sum_{m=1}^{N} d_m s_{M+m}(\mathbf{r},\phi+\delta_{\mathrm{PZT}},\alpha_{M+m})}{\sum_{m=1}^{M} n_m s_m(\mathbf{r},\phi,\alpha_m)\sum_{m=1}^{M} d_m s_m(\mathbf{r},\phi,\alpha_m) + \sum_{m=1}^{N} n_m s_{M+m}(\mathbf{r},\phi+\delta_{\mathrm{PZT}},\alpha_m)\sum_{m=1}^{N} d_m s_{M+m}(\mathbf{r},\phi+\delta_{\mathrm{PZT}},\alpha_{M+m})}. \tag{7}$$

The shift δ_{DPSA} is affected by the various systematic and random errors of the DPSAs. A histogram of the whole field image is obtained for each value with its average value and its typical deviation. Thus, a calibration line can be constructed with the values of δ_{PZT} and δ_{DPSA}. For example, Fig. 3 shows the line calibration drawn making use of Schwider-Hariharan[14,15] DPSA. The well-known compensatory capacities of this algorithm justify the regression coefficient R, one with a nearly 99% significance level. A test statistic for the F-test on the regression model provides a value of 6,881.666. Therefore, a significant linear regression relationship between the variables is provided. Finally, the p-value for the F-statistic of the linear relationship is equal to zero.

4 External Cavity Diode Laser Stabilization Using a Laser Mode Locking Technique

External cavity diode lasers (ECDL) can be used as an alternative to He-Ne gas lasers in dimensional metrology. These lasers take advantage of efficient, low-cost diode lasers and use frequency selective feedback to achieve narrow line width and tunability. Typically, the feedback is obtained through a diffraction grating in the Littrow configuration, and the narrow line width is achieved by a mode-locking technique using a reference gas cell, such as what is currently

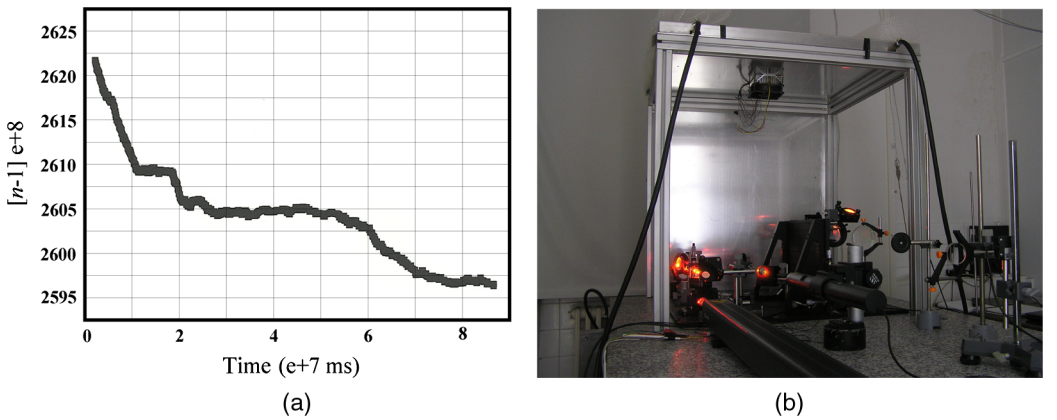

Fig. 2 Refractive index calculation stability (a) and real view of the experimental setup (b).

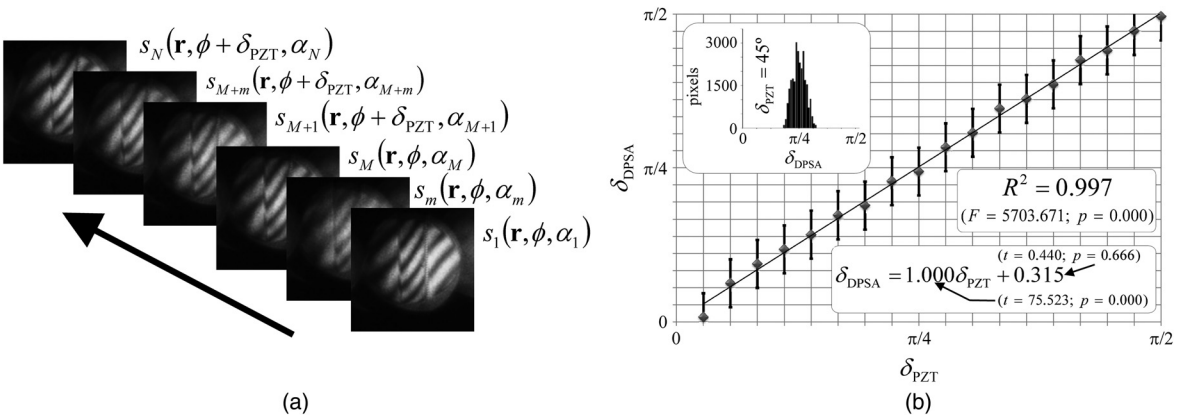

Fig. 3 $M+N$ phase-shifted patterns (a) and an example of the calibration line for δ values in the interval $[0,\pi/2]$ (b).

used in fundamental physics labs to cool atoms using magneto-optical traps.[16–18]

The experimental setup is shown in Fig. 4, and the laser beam is split in two probe beams and a saturating beam. The first two beams are shifted in the same direction and are received by the photodetectors, whereas the third one is shifted in the opposite direction to cross one of the others. This third beam, which is much more powerful than the others, is used to attain the saturation of the cell, avoiding the laser Doppler effect, which limits the line width to 1 ppm of the desired frequency. Frequency variations of the laser are turned into amplitude variations on the photodetector, due to the selective absorption of the gas cell. This electronic signal is controlled by the Moglabs DLC-202 electronics system, which drives a grating assembled on a piezoelectric actuator. Depending on the intensity differences detected by the photodetector, the controller can change the grating angle, which tunes the frequency of the probe beam. With this procedure, the bandwidth of the laser diodes can be reduced[19–21] to less than 1 MHz.

The line width is sensitive to the variations of the cavity length, laser diode temperature and current, feedback and gratting efficiency, and optical system alignment. Therefore, to avoid mechanical vibrations and temperature gradients and to keep the laser resonant cavity at a constant temperature, an encapsulated mechanical system was designed.

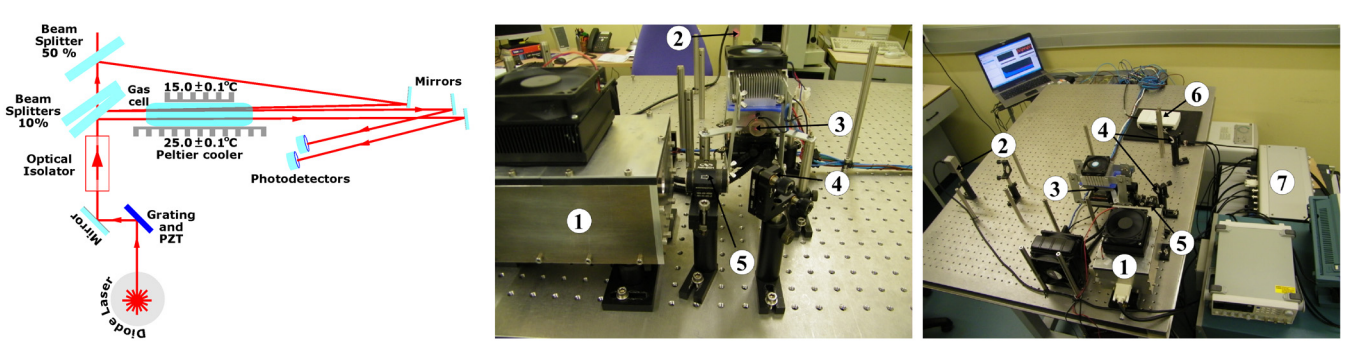

Fig. 4 Optical diagram and photography of the experimental setup: ECDL (1), photodetectors (2), iodine cell (3), beam splitters (4), optical isolator (5), DAQ (6), electronic controller (7).

This system was temperate and isolated, and it allowed the grating assembly, the mirror reflector, and the piezoelectric actuator to be integrated in the same module. This design reduces the mode spacing of the external cavity, while the cavity length can be tuned facing the laser mode hop.[22–24] The mechanical device depicted in Fig. 5 consists of a red laser diode at 635 nm (HL6344G) coupled to a collimator tube (Thorlabs LT230P-B), which incorporates a mounted aspheric lens (Thorlabs A230TM-A, $f = 4.51$ mm NA $=$ 0.54, 350 to 700 nm). These elements are mounted to a piece of aluminum connected to a Peltier cell (Global Componet Sourcing ET-131-10-13-S-RS, 36W 4A), and the temperature is measured by a temperature sensor (Texas Instruments AD592). In addition, there is a piece of stainless steel supporting the grating (Thorlabs GR25-1850, 18, 00 l/mm), the mirror, and two piezoelectric actuators. This mirror is parallel to the diffraction grating and produces a fixed output beam regardless of the changes in the cavity length and grating angle.[19] The two different piezoelectric actuators, a stack (Noliac CMAP04) and a disc (Steminc SMD20T08F2500R), are responsible for changing the cavity length and seeking a better frequency response function in the control feedback. Moreover, three high-precision adjustment screws (Newport AJS100) are used to align the grating with the laser diode to achieve a fine alignment of the first diffraction order. Finally, the whole ECDL system is mounted to a thick invar 36 plate to provide inertial and thermal damping, and it is isolated from the environment through an aluminum box.

Furthermore, to assure good stability in the reference frequency given by the iodine cell, temperature stabilizing was performed on it. A thermal conditioning system was developed based on four Peltier cells (Melchor CP1.4-127-045-RTV), two SuperCool PR-59 controllers, and two fans (Coisar H80 and Fisher SK100-75-SA), as depicted in Fig. 6. To guarantee the accuracy of this thermal stabilization system, the NTC temperature sensors of the PID controllers (SuperCool PR-59) were calibrated by LOMG with deviations and uncertainties lower than 0.1ºC. This system allows the cell to be stabilized with better parameters than the required specifications of 25.0 ± 5°C for the cell and 15.0 ± 0.2°C for the cold finger,[19,25] as shown in Fig. 7, over a period of 6 h.

This ECDL experimental setup was tested on the laser fluorescence phenomenon (as shown in Fig. 6), which is triggered by de-excitation of the iodine after having been excited by the laser at its absorption line. Figure 8 presents several absorption lines around 632.9 nm [R(127) 11-5 a16 transition],[19,25] detected by the photodetector when a triangular voltage sweep of the cavity was made by the stack piezoelectric. For this sweep, an interval between two peaks is shown in these figures to assess the quality of the system. Figure 8(b) shows the laser mode hops, which disguise the absorption lines, using the previous ECDL version without the mechanical system. However, Fig. 8(c) depicts the absorption lines achieved with the ECDL presented in this work. The downward dashed arrows mark two iodine transitions, labelled as a_n, because it was not possible to measure the absorption lines, since low-resolution equipment does not allow the spectral lines to be evaluated with the required precision. However, this equipment can measure the line width of the absorption lines, whereas the laser is stabilized. Also, Fig. 8(d) shows the error in the frequency measured during a mode-locking frequency technique using Fourier transform analysis. The diode frequency remained stable for a period of 5 h with a line width of 0.2 ppm. Therefore, this technique is suitable for adapting laser diodes as a reference frequency in metrological applications. The next step will enhance the stability of the ECDL, adjust the cavity parameters to avoid doing new alignments when a diode is changed, and measure the wavelength of the laser to know the accurate iodine transition fixed by the laser.

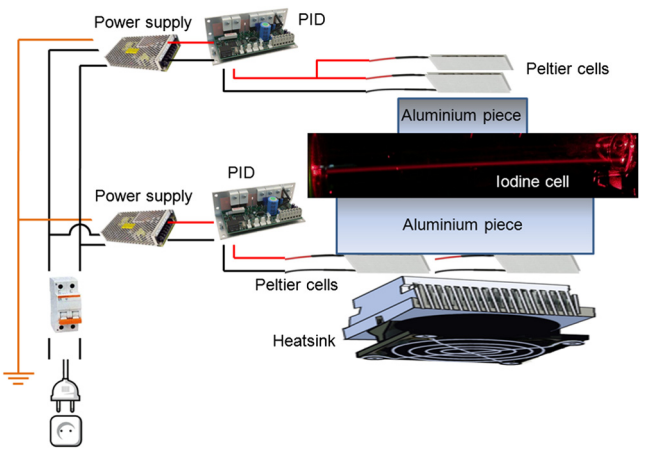

Fig. 6 Scheme of the temperature controller for the iodine cell.

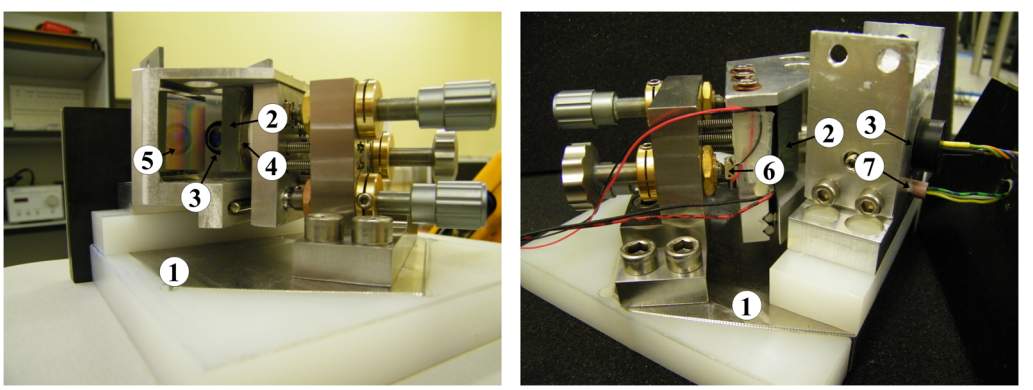

Fig. 5 Mechanical system of the external cavity diode laser (ECDL): Invar plate (1), grating (2), laser diode (3), PZT disc (4), mirror (5), PZT stack (6), temperature sensor (7).

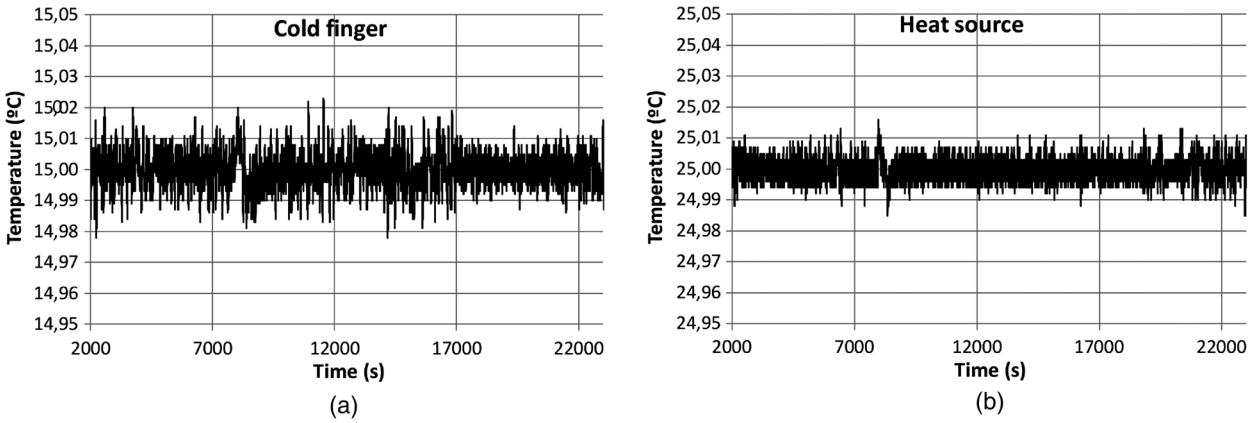

Fig. 7 Temperature stabilization of the iodine cell: (a) cold finger and (b) heat source.

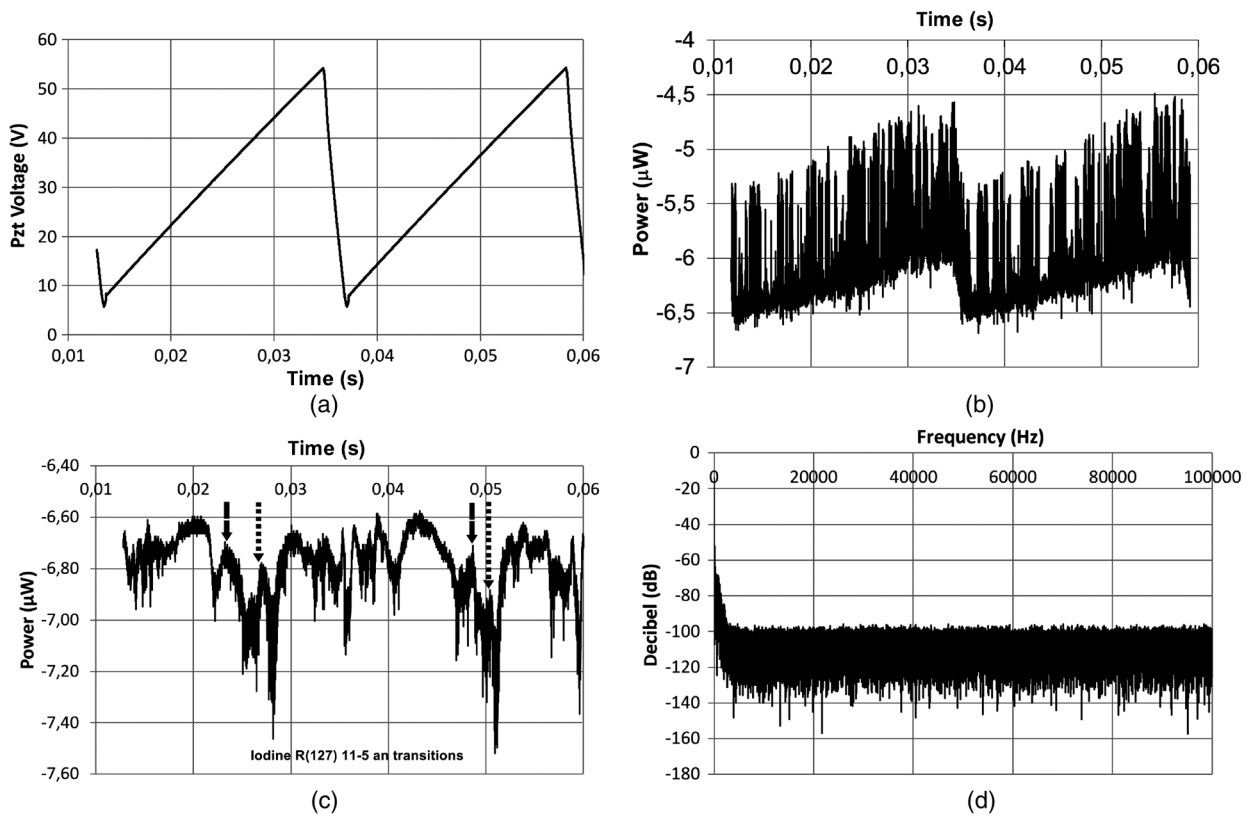

Fig. 8 (a) Triangular voltage sweep of the resonant cavity, (b) mode hops of the previous ECDL setup, (c) iodine absorption lines detected by the ECDL presented in this work and marked by the downward dashed arrows, and (d) frequency spectrum of the stabilized laser diode.

5 Summary and Conclusions

This work shows several aspects of the process of designing, constructing, and calibrating of a new multiple-wavelength Twyman-Green interferometer for the calibration of GBs. This interferometer has a custom developed automatic evaluation system based on optomechanical modulation, and the refractive index of the air was calculated using Edlén's equation to obtain the final length value. The main features of the interferometer are described, including the phase-shifting and image acquisition system. A procedure for the calibration is developed, and the experiments are carried out to stabilize a diode laser as a light source. We are planning to design a complete control loop that involves hardware and software developments to achieve the maximum performance of the stabilization process using low-cost components. The aim is to attain an automated GB dimensional measurement system employing robust and cheap laser diodes as light sources. The results obtained by calculating the refractive index of air and the optomechanical modulator show a high level of theoretical-experimental correlation.

Acknowledgments

The authors are grateful to the Spanish Ministry for Education and Science for funding the DPI2008-06818-C2-01 & 02/DPI Project.

References

1. J. E. Decker and J. R. Pekelsky, "Uncertainty evaluation for the measurement of gauge blocks by optical interferometry," *Metrologia* **34**(6), 479–493 (1997).
2. B. Edlén, "The refractive index of air," *Metrologia* **2**(2), 71–80 (1966).
3. K. P. Birch and M. J. Downs, "An updated Edlén equation for the refractive index of air," *Metrologia* **30**(3), 155–162 (1993).
4. K. P. Birch and M. J. Downs, "Correction to the updated Edlén equation for the refractive index of air," *Metrologia* **31**(4), 315–316 (1994).
5. J. E. Decker, R. Schödel, and G. Bönsch, "Considerations for the evaluation of measurement uncertainty in interferometric gauge block calibration applying methods of phase step interferometry," *Metrologia* **41**(3), L11–L17 (2004).
6. M. Miranda and B. V. Dorrío, "Fourier analysis of two-stage phase-shifting algorithms," *J. Opt. Soc. Am. A* **27**(2), 276–285 (2010).
7. M. Miranda and B. V. Dorrío, "Monte Carlo based techniques of two-stage phase shifting algorithms," *Opt. Lasers Eng.* **49**(3), 439–444 (2011).
8. M. Miranda et al., "Characteristic polynomial theory of two-stage phase shifting algorithms," *Opt. Lasers Eng.* **50**(4), 522–528 (2012).
9. J. A. Stone and J. H. Zimmerman, "Index of refraction of air," NIST 28, December 2011, http://emtoolbox.nist.gov/Wavelength/Edlen.asp (10 January 2013).
10. M. Born and E. Wolf, *Principles of Optics*, p. 291, Pergamon Press Ltd., Cambridge (1980).
11. P. E. Ciddor, "Refractive index of air: 3. The roles of CO_2, H_2O, and refractivity virials," *Appl. Opt.* **41**(12), 2292–2298 (2002).
12. B. V. Dorrío and J. L. Fernández, "Phase-evaluation methods in whole-field optical measurement techniques," *Meas. Sci. Tech.* **10**(3), 33–35 (1999).
13. V. Álvarez-Valado et al., "Testing phase-shifting algorithms for uncertainty evaluation in interferometric gauge block calibration," *Metrologia* **46**(6), 637–645 (2009).
14. J. Schwider et al., "Digital wave-front measuring interferometry: some systematic error sources," *Appl. Opt.* **22**(22), 3421–3432 (1983).
15. P. Hariharan, B. F. Oreb, and T. Eiju, "Digital phase-shifting interferometry: a simple error-compensating phase calculation algorithm," *Appl. Opt.* **26**(13), 2504–2506 (1987).
16. K. B. McAdam, A. Steibach, and C. Wieman, "A narrow-band tunable laser diode system with gratting feedback, and saturated absortion spectrometer for Cs and Rb," *Am. J. Phys.* **60**(12), 1098–1111 (1992).
17. M. C. Wieman and G. Flowers, "Inexpensive laser cooling and trapping experiment for undergraduate laboratories," *Am. J. Phys.* **63**(4), 317–330 (1995).
18. "Research groups working with atom traps," University of Innsbruck, 31, March 2007, http://www.uibk.ac.at/exphys/ultracold/atomtraps.html (10 January 2013).
19. H. Talvitie, M. Merimaa, and E. Ikonen, "Frequency stabilization of a diode laser to Doppler-free spectrum of molecular iodine at 633 nm," *Opt. Commun.* **152**(1–3), 182–188 (1998).
20. C. J. Hawthorn, K. P. Weber, and R. E. Scholten, "Littrow configuration tunable external cavity diode laser with fixed direction output beam," *Rev. Sci. Instrum.* **72**(12), 4477–4479 (2001).
21. R. W. P. Drever, "Laser phase and frequency stabilization using an optical resonator," *Appl. Phys. B: Lasers Opt.* **31**(2), 97–105 (1983).
22. C. Ye, *Tunable External Cavity Diode Lasers*, World Scientific, Texas A & M University (2004).
23. J. M. W. Kruger, "A novel technique for frequency stabilizing laser diodes," Postgraduate Diploma in Science, University of Otago (1998).
24. S. D. Saliba et al., "Mode stability of external cavity diode lasers," *Appl. Opt.* **48**(35), 6692–6700 (2009).
25. T. J. Quinn, "Practical realization of the definition of the metre, including recommended radiations of other optical frequency standards," *Metrologia* **40**(2), 103–133 (2003).

Javier Diz-Bugarín graduated as a telecommunications engineer from the University of Vigo, Spain, in 1994. He has worked as a fellow in the Applied Physics Department in several projects related to optical metrology, and he is currently working on a PhD in gauge block calibration. He also has experience in electronics R&D. He is also working as a teacher of electronics, and he has written several papers about electronics design and renewable energies.

Benito V. Dorrío received his BSc degree in physics in 1990 from the University of Santiago de Compostela, Spain, and his PhD in physics in 1996 from the University of Vigo, Spain. Since 1998, he has held a permanent research position as an assistant professor at the University of Vigo. He has coauthored more than 50 international scientific publications. His research interests include fringe analysis, interferometry, and phase evaluation methods.

Jesús Blanco-García received his doctoral degree in physics in 1992, with a thesis on holographic interferometry, from the University of Santiago de Compostela, Spain. He currently teaches physics at the University of Vigo, Spain. His main research subjects are holographic interferometry, moiré methods, ESPI, interferometer fringe analysis, and physics education.

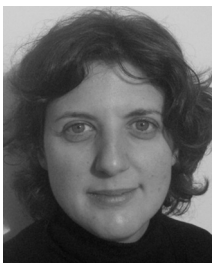

Marta Miranda obtained her BSc in physics (optoelectronics) from the University of Santiago de Compostela, Spain, in 2003. Then she joined the Applied Physics Department at the University of Vigo, Spain, to work on the analysis of differential phase shifting algorithms to get her PhD in 2010. Nowadays, she is developing new tools to analyze the behavior of phase evaluation algorithms for optical metrology.

Ismael Outumuro graduated in 2006 with a degree in physics from the University of Vigo, Spain. Soon afterward, he joined the Metrology Laboratory of Galicia, Spain, where is currently working in dimensional metrology, in particular laser interferometry and coordinate measurement machines. He is enrolled in a PhD program in laser applications in metrology.

Jose Luis Valencia is a researcher at the Metrology Laboratory of Galicia, Spain. He earned his MSc in 2000 and his PhD in 2005 in physics from the University of Vigo, Spain. He has worked at the National Physical Laboratory, UK, as a guest researcher from 2008 to 2010 in the area of dimensional nanometrology. His current areas of interest are atomic force microscopy and laser interferometry.